

Original Research Article

Imaging spectrum of renal masses on multi-slice computed tomography

Dipak R. Thakor¹, Yashpal R. Rana^{2*}, Megha M. Sheth²

¹Department of Radiology, Medimax Imaging Centre, Ahmedabad, Gujarat, India

²Department of Radiology, Radiscan Diagnostics, Ahmedabad, Gujarat, India

Received: 10 August 2020

Accepted: 14 September 2020

*Correspondence:

Dr. Yashpal R. Rana,

E-mail: yashpalmy2@gmail.com

Copyright: © the author(s), publisher and licensee Medip Academy. This is an open-access article distributed under the terms of the Creative Commons Attribution Non-Commercial License, which permits unrestricted non-commercial use, distribution, and reproduction in any medium, provided the original work is properly cited.

ABSTRACT

Background: Multi-slice computed tomography (MSCT) is the mainstay for preoperative assessment of many complex renal masses in current clinical practice. Benign renal processes may simulate malignant renal tumors and could be defined correctly by CT. MSCT has also an important role in tumor staging. The purpose of this article is to understand the imaging spectrum of renal masses on MSCT and assess the usefulness of CT in surgical planning and management.

Methods: Studied 500 patients with suspected renal lesions who underwent MSCT during the period July 2017 to July 2020 at state-of-art imaging center. CT imaging was done in those patients in whom clinical examination and ultrasonography (USG) revealed possibility of diagnosis of renal masses for further detailed evaluation and deciding management.

Results: Out of 500 total subjects, the common age group in this study is 51 to 60 years (25%). Male preponderance (59%) was noted. The most common presentation was pain (84%) followed by lump (29.4%) and haematuria (17.8%). Malignant masses (51%) were more common followed by benign (39%) and inflammatory masses (10%) respectively. Renal cell carcinoma has more incidence (30%) followed by simple cyst (20%). Calcification (19.6%), perinephric extension (78%) and vascular invasion (21.5%) are more common in malignant masses.

Conclusion: MSCT is the modality of choice for the diagnosis of renal masses and deciding management approach in current practice. Detection of tumoral spread, invasion of surrounding organs and vascular structure are better with CT. MSCT also has a role in postoperative follow-up of renal masses.

Keywords: Renal masses, MSCT, Renal cell carcinoma, Simple cyst

INTRODUCTION

Renal masses constitute more than or at least 50% of the abdominal masses in children as well as in adults.^{1,2} They are difficult to differentiate from other masses on a clinical basis only hence radiological examination becomes an important path to reach the diagnosis before surgery. MSCT is the mainstay for pre-operative assessment of many complex renal masses in current clinical practice. MSCT is widely accepted as the preferred imaging technique for suspected renal tumors, and also has an important role in tumor staging.³⁻⁶ Benign renal processes, including cystic disease, renal infection,

and benign tumors may simulate malignant renal tumors and could be defined correctly by CT. The improvements in CT technique and increased use of cross-sectional imaging have facilitated the detection of small or previously undiagnosed renal masses. Though magnetic resonance imaging (MRI) has greater capabilities, it is time-consuming, still less widely available, and may require a lengthy period of sedation; hence its use in pediatric subjects, seriously ill or uncooperative patients is often limited.^{7,8} On the other hand, MSCT offers the advantages of short acquisition times and widespread availability.

Although ultrasound is considered as an initial imaging modality of choice, it is limited in the reliable assessment because of operator dependency, limited capability to differentiate various lesions, and limited evaluation of the extension of the lesions. Cross-sectional imaging with MSCT or magnetic resonance (MR) helps overcome these limitations. Radiologists should become familiar with the variety of renal lesions, their imaging appearances, and various management and surgical procedures. MSCT also plays a crucial role in the postoperative follow-up of the masses.

The objective of this article is to understand the imaging spectrum of various renal masses on MSCT and to assess the usefulness of CT scans in surgical planning and management.

METHODS

This is a retrospective, observational study of 500 patients with suspected renal lesions who underwent MSCT during the period July 2017 to July 2020 at our high-volume state-of-art diagnostic imaging centre. Ethics committee approval was obtained for the study. Details of MSCT scan parameters and various phases on MSCT imaging are as shown in table 1 and table 2.

Inclusion criteria for the study included USG is the initial modality of choice. MSCT imaging was done in those patients in whom clinical examination and USG revealed primary/suspicious diagnosis of renal masses for further detailed evaluation and deciding management planning. Blood investigations like-HIV, HBsAg, Serum creatinine of all patients were mandatory. Patients were advised to come on an empty stomach for at least six hours for a CT scan. Relevant history of an allergic reaction, illness, and significant clinical findings of all patients were recorded. Previous investigations were reviewed.

In exclusion criteria excluded patients with known contrast allergy; Patients with altered renal status (creatinine >2 mg/dl); Patients with hyperthyroidism and pregnancy; Patients with cardiac arrhythmias and unable to hold breath; Patients contraindicated for beta-blockers i.e. severely deranged left ventricular ejection fraction, history of bronchial asthma, arterio-ventricular conduction block etc.

Various image reformatting techniques including curved multi-planar reconstruction (c-MPR), maximum intensity projection (MIP), and 3D volume-rendering technique (VRT) are used to get all the clinically relevant information. It is important to examine source images as well apart from reconstructed images; as some information might be missed by interpreting only reconstructed images.

RESULTS

Found non-invasive MSCT to be highly sensitive as well as specific for the diagnosis of renal masses. Out of 500 total subjects, the maximum incidence of renal masses in our study is between 51 to 60 years (25%) (Table 3). The incidence shows male preponderance (59%) (Table 4). The most common presentation was pain (84%) followed by a lump (29.4%) and haematuria (17.8%) (Table 5). Malignant masses (51%) were more common followed by benign (39%) and inflammatory masses (10%) respectively (Table 6). Renal cell carcinoma has more incidence (30%) followed by a simple cyst (20%) (Table 7). As shown in table-8, calcification (19.6%), perinephric extension (78%) and vascular invasion (21.5%) are more common in malignant renal masses. Fat is more common in benign tumors (20.5%) while lymphadenopathy is more common in inflammatory masses (27%).

Table 1: MSCT technique parameters.

Scanner	16 slice brilliance (Philips Healthcare, USA)
Contrast medium and amount	Non-ionic, 1-1.5 ml/kg Saline chaser (half that of contrast amount)
Flow rate (ml/sec)	4
Scan timing	Bolus tracking, Scan triggered at 100 HU
Peak kilovoltage (kVp)	100/120
Effective mAs	175-200

Table 2: Various phases on MSCT imaging.

Phase	Time delay after contrast injection (Seconds)	Importance
Arterial phase	20	Depict renal arteries
Parenchymal phase	90-120	Lesion characterization and demonstrating the collecting system anatomy.
Excretory phase	180-30	Delineate the relationship of centrally located mass with collecting system and evaluating the urothelial masses.

Table 3: Age-wise distribution of patients in the study.

Age (years)	Number of patients (%)
0-1	25 (5)
1-10	65 (13)
11-20	5 (1)
21-30	35 (7)
31-40	45 (9)
41-50	95 (19)
51-60	125 (25)
Above 60	105 (21)
Total	500

Table 4: Sex wise distribution of patients in the study.

Gender	Number of patients (%)
Male	295 (59)
Female	205 (41)

Table 5: Clinical symptoms of patients in the study.

Clinical symptoms	Number of patients (%)
Lump	147 (29.4)
Haematuria	89 (17.8)
Pain	421 (84.2)

Table 6: Distribution of renal masses according to etiology.

Masses	Number of patients (%)
Inflammatory	50 (10)
Benign	195 (39)
Malignant	255 (51)

Table 7: Different renal masses frequency in study.

Diagnosis	Number of patients (%)
Simple cortical cyst	100 (20)
Complex renal cyst	15 (3)
Adult polycystic kidney	20 (4)
Hydatid cyst	5 (1)
Angiomyolipoma	35 (7)
Pseudotumour	5 (1)
Abscess	30 (6)
Xanthogranulomatous pyelonephritis	5 (1)
Tuberculosis	10 (2)
Oncocytoma	10 (2)
Renal cell carcinoma	150 (30)
Wilms tumor	60 (12)
Mesoblastic nephroma	10 (2)
Transitional cell carcinoma	10 (2)
Lymphoma	10 (2)
Metastasis	5 (1)
Sarcoma	5 (1)
Recurrence	15 (3)

Table 9: Broad classification of renal masses.

Benign		Malignant			
Epithelial	Mesenchymal	Epithelial	Mesenchymal	Embryonal tumors	Secondary
Adenoma	Fibroma	Adenocarcinoma	Sarcoma	Wilm's tumor	Leukemia, Lymphoma, Metastasis from the breast, bronchus, stomach, melanoma, etc.
	Myoma				
	Lipoma				
	Angioma				
	Angiomyolipoma				
	Reninoma				
	Mixed mesenchymal tumors (Hamartoma)				
Tumors of the renal pelvis					
Benign	Malignant				
Non-epithelial	Epithelial		Non-epithelial (Mesenchymal)	Secondary	
	Transitional cell carcinoma, Squamous cell carcinoma, Adenocarcinoma		Mesenchymal sarcoma		
Renal cysts					
Simple renal cyst	Polycystic renal disease - Infantile - Adult	Renal dysplasia -Multicystic kidney -Focal and segmental cystic dysplasia	Medullary cystic disease -Medullary sponge kidney -Uremic medullary cystic disease	Miscellaneous	
				-Multilocular renal cysts -Calyceal diverticula -Cysts of infectious origin -Cysts associated with neoplastic disease -Traumatic cysts: intrarenal hematoma -Pararenal Pseudocyst: urinoma	
Inflammatory/Infectious masses					
Xanthogranulomatous pyelonephritis					
Renal abscess					
Renal tuberculosis					
Renal hydatid					

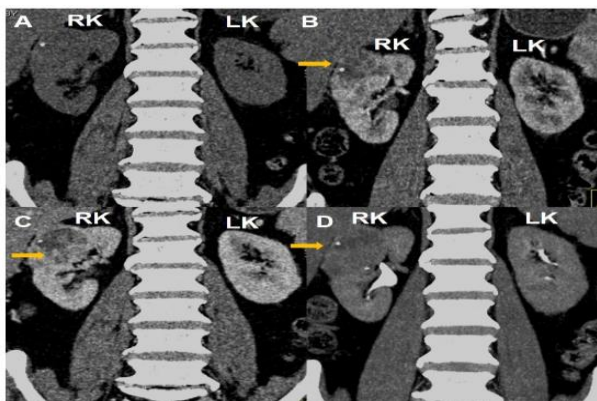


Figure 1: Renal cell carcinoma.

Coronal CT images shows (A): Plain non-contrast, (B): Nephrographic phase, (C) Cortico-medullary phase, and (D) Delayed phase show well-encapsulated, exophytic, heterogeneously enhancing necrotic mass lesion in

relation to the upper-mid pole of the right kidney. RK = Right kidney. LK = Left kidney.

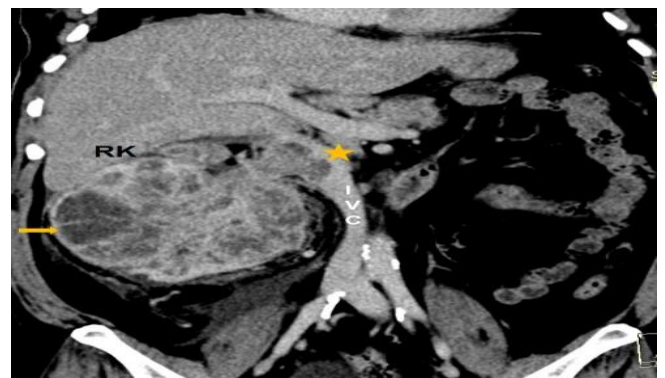


Figure 2: Renal cell carcinoma with tumoral thrombus in the right renal vein and IVC.

Coronal CT image shows large, well-defined, a heterogeneously hyper-enhancing necrotic mass lesion in the right kidney (yellow arrow) with tumoral thrombus in right renal vein and IVC (yellow star). RK = Right kidney. LK = Left kidney. IVC = Inferior Vena Cava.

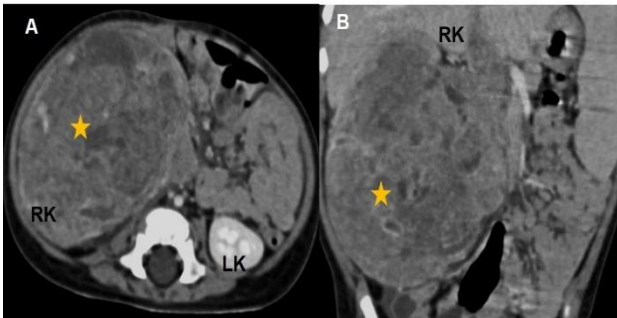


Figure 3: Wilm's tumor.

The image shows (A): Axial, (B): coronal CT images show a large, well-defined, heterogeneous necrotic mass lesion in the right kidney (yellow star) with a mass effect on surrounding structures. RK = Right kidney. LK = Left kidney.

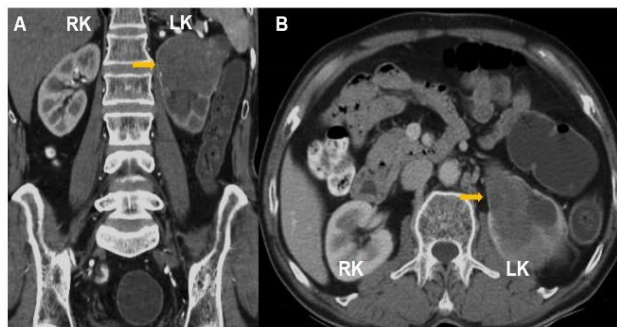


Figure 4: Transitional cell carcinoma.

The image shows (A): Coronal, (B): axial CT images large, well-defined, heterogeneous mass lesion involving left the pelvicalyceal system and left pelviureteric junction (yellow arrow). RK = Right kidney. LK = Left kidney.

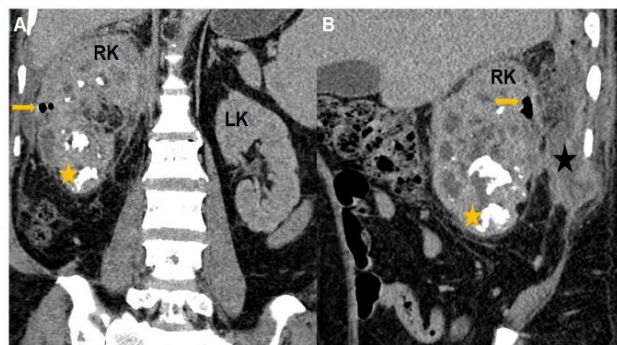


Figure 5: Xanthogranulomatous pyelonephritis.

The image shows (A): Coronal, (B): sagittal CT images show enlarged right kidney with perinephric collection (black star), multiple radiodense calculi (yellow star), and air foci (yellow arrow) confirming changes of xanthogranulomatous pyelonephritis. RK = Right kidney. LK = Left kidney.

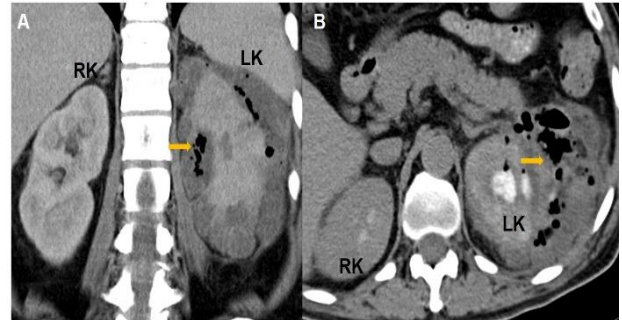


Figure 6: Emphysematous pyelonephritis.

The image shows (A): Coronal, (B): axial CT images show enlarged left kidney with the perinephric collection and air foci (yellow arrow) confirming changes of emphysematous pyelonephritis. RK = Right kidney. LK = Left kidney.

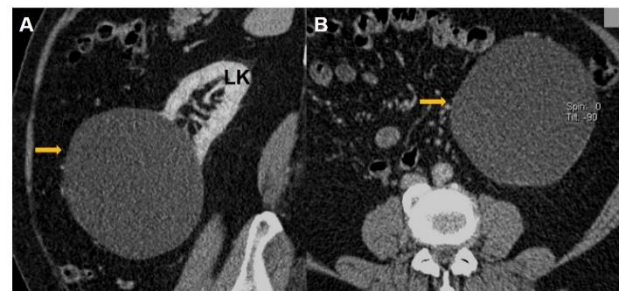


Figure 7: Simple cyst.

The image shows (A): Sagittal, (B): axial CT images show a large, well-defined, exophytic, cystic lesion in relation to the lower pole of the left kidney (yellow arrow). LK = Left kidney.

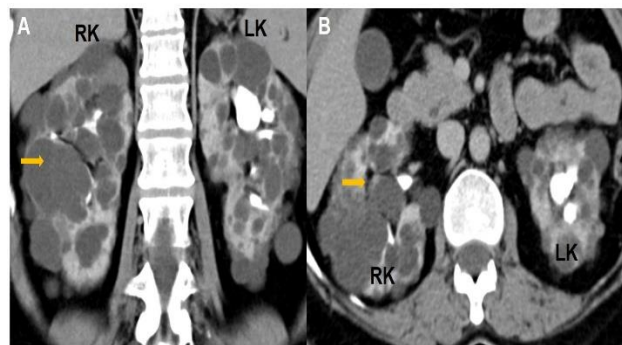


Figure 8: Autosomal dominant polycystic kidney disease.

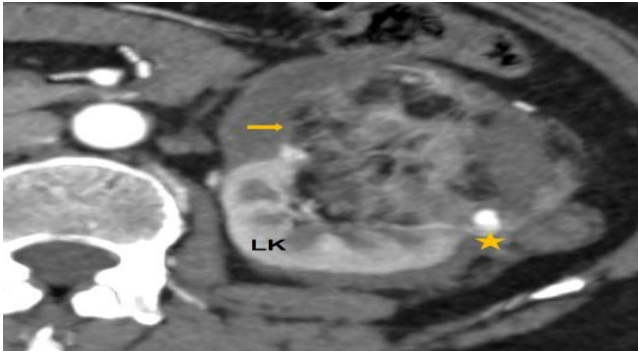


Figure 9: Angiomyolipoma.

The image shows that (A): Coronal, (B): axial CT images show multiple varying size cysts (yellow arrow) in both kidneys, replacing entire renal parenchyma. RK = Right kidney. LK = Left kidney.

The image shows that axial CT image shows large, well-defined, heterogeneous mixed density mass lesion with fatty areas within involving the left kidney (yellow arrow). The yellow star represents a saccular aneurysm of the lobar renal artery. RK = Right kidney. LK = Left kidney.

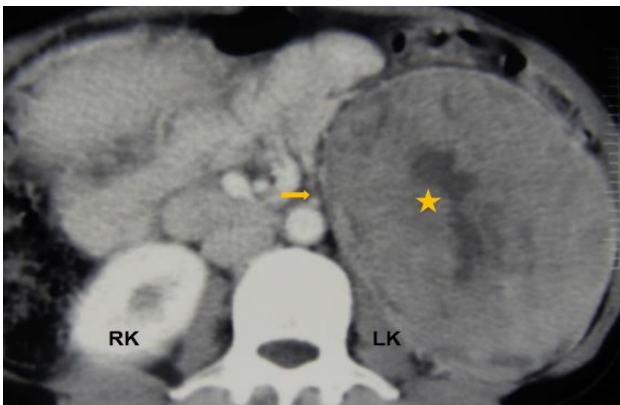


Figure 10: Oncocytoma.

Axial CT image shows a large, well-defined, heterogeneous mass lesion in the right kidney (yellow arrow) with a central scar (yellow star). RK = Right kidney. LK = Left kidney.

DISCUSSION

Renal masses are broadly classified as cortical renal tumors, tumors of the renal pelvis, renal cysts, and inflammatory/infections masses (Table-9).⁹⁻¹² MSCT is the mainstay for pre-operative assessment of many complex renal masses in current clinical practice. The improvements in CT technique and increased use of cross-sectional imaging have facilitated the detection of small or previously undiagnosed renal masses.

Renal cell carcinoma is the most common primary renal cancer and MSCT is the primary modality for detection,

diagnosis, and staging of RCC.¹³⁻¹⁵ On the non-contrast scan, they may appear hypodense, isodense, or hyperdense as compared with normal renal parenchyma and after administration of contrast material most enhance but to a lesser extent than renal parenchyma. This feature is best seen in the nephrographic phase. Enhancement is often heterogeneous due to tumor necrosis or haemorrhage (Figure 1). Perinephric invasion is suggested by perinephric soft tissue mass at least 1 cm in diameter. Venous tumoral invasion can be identified on a CT scan if there is an identifiable enhancing thrombus in the renal vein or inferior vena cava (Figure 2).

Wilm's tumor presents between the ages of 1 to 5 years. On CT, it usually presents as a large, spherical intrarenal mass, very often with a rim of compressed renal parenchyma or pseudo capsule surrounding it. The tumor is less dense than normal renal parenchyma on contrast-enhanced CT scans (Figure 3).^{16,17} CT may also identify bilateral Wilm's tumor and liver and pulmonary metastasis.

90% of pelvicalyceal cancers are transitional cell carcinomas and have peak frequency in the 6th and 7th decades of life with male preponderance. CT helps in establishing the extent of renal parenchymal invasion including the perinephric and periureteral extents of tumour (Figure 4).¹⁸ CT demonstrates collecting system filling defects with smooth, lobulated, or irregular margins.

Among secondary neoplasms of the kidney, renal lymphoma shows different CT patterns -multiple renal mass, solitary mass, renal invasion from contiguous retroperitoneal disease, perirenal disease and diffuse renal infiltration. Metastasis to the kidney in order of frequency is from lung carcinoma, breast carcinoma, and carcinoma of another kidney. The most common pattern on CT is that of multiple discrete bilateral lesions.²¹ Solitary exophytic masses are most common in colon cancer.

Inflammatory renal masses include xanthogranulomatous pyelonephritis, renal abscess, tuberculosis, and hydatid disease. Xanthogranulomatous pyelonephritis is an unusual suppurative granulomatous reaction to chronic infection, often in the presence of chronic obstruction from a calculus, stricture, or tumor. CT shows diffuse reniform enlargement with ill-defined central low attenuation, cortical thinning, staghorn calculus, and unilateral decrease or absence of excretion of contrast material (Figure 5).²² Perinephric extension of the inflammatory process is common. A renal abscess results most commonly as a sequela of severe, acute pyelonephritis. On CT, the abscess appears as a heterogeneous low-attenuation mass with often an irregular, enhancing wall (Figure 6). Renal tuberculosis is usually due to hematogenous seeding from pulmonary disease. The classical CT findings are multifocal caliectasis, due to irregular infundibular strictures.

Parenchymal scars may be seen in advanced cases. Ultimately, the kidney may become small, densely calcified, and non-functioning: the so-called auto-nephrectomy. Renal hydatid appears as uniloculated or a multiloculated cyst that may have rim enhancement on CT.

Common cystic renal diseases include Autosomal recessive polycystic kidney disease (ARPKD), Autosomal dominant polycystic kidney disease, multicystic dysplastic kidney (MCDK), and simple cysts (Figure 7 and 8).

Angiomyolipoma lesions are composed of heterogeneous tissues, including blood vessels, adipose tissue, and smooth muscle, and may present as sporadic cases or in association with tuberous sclerosis (Figure 9). Oncocytoma is a well-circumscribed, benign mass with a central stellate scar (Figure 10).

In this study, out of 500 patients, 30% were renal cell carcinoma, 20 % simple cysts and 12 % were Wilm's tumor. A study by Daniel Jr and Hartman et al showed that among the renal masses 61.3% were simple cysts, 20.6% were renal cell carcinoma, 1.2% were abscesses and Wilm's was the diagnosis in less than 1% cases.¹⁵ Warren, Kelalis and Utz in their study showed the haematuria to be present in 40-60% of cases, flank pain was the presenting symptom in about 50% of cases, the palpable abdominal mass was present in 35-40% of cases and fever in 15-25% of cases, weight loss in about 30% of cases. This is very much similar to the present study.²³

Malignant masses (51%) were more common followed by benign (39%) and inflammatory masses (10%) respectively in this study, Lopez-Beltran et al also demonstrated a nearly same incidence of renal masses.⁹ Renal cell carcinoma has more incidence (30%) followed by simple cyst (20%).¹² Calcification (19.6%), perinephric extension (78%) and vascular invasion (21.5%) are more common in malignant renal masses.¹⁵

CONCLUSION

Nowadays, MSCT is the modality of choice for the diagnosis of renal masses. Being very specific, not only it confirms the diagnosis but also help differentiating between solid versus cystic or benign versus malignant masses. Detection of tumoral spread as well as invasion of surrounding organs and vascular structure is better with CT. Thus, it helps to decide the management approach. MSCT also has a role in postoperative follow-up of patients with renal masses. In current practice, despite its radiation issue, CT is the prime investigation in the evaluation of renal masses.

Funding: No funding sources

Conflict of interest: None declared

Ethical approval: The study was approved by the Institutional Ethics Committee

REFERENCES

1. Jemal A, Siegel R, Xu J, Ward E. Cancer statistics. *CA Cancer J.* 2010;60:277-300.
2. David Sutton: *The Textbook of Radiology and Imaging*, Edinburgh, London, New York, Churchill Livingstone, 7th edi. 2002;929-87.
3. Mileto A, Nelson RC, Paulson EK, Marin D. Dual-Energy MDCT for Imaging the Renal Mass. *AJR Am J Roentgenol.* 2015;204:640-7.
4. Kaza RK, Platt JF. Renal applications of dual-energy CT. *Abdom Radiol.* 2016;41:1122-32.
5. Sheth S, Fishman EK: Multidetector row CT of the kidneys and urinary tract: Techniques and applications in the diagnosis of benign diseases. *Radiographics.* 2004;24(2):20.
6. Birnbaum BA, Jacobs JE, Ramchandani P. Multiphase renal CT: Comparison renal mass enhancement during corticomedullary and nephrogenic phases. *Radiology.* 1998;200(3):753-8.
7. Pedrosa I, Sun MR, Spencer M, Genega EM, Olumi AF, Dewolf WC et al. MR imaging of renal masses: Correlation with findings at surgery and pathologic analysis. *Radiographics.* 2008;28:985-1003.
8. Dyer R, Di Santis DJ, McClennan BL. Simplified imaging approach for evaluation of the solid renal mass in adults. *Radiology.* 2008;247:331-43.
9. Lopez-Beltran A, Scarpelli M, Montironi R, Kirkali Z. 2004 WHO classification of the renal tumors of the adults. *Eur Urol.* 2006;49:798-805.
10. Hélénon O, Eiss D, Debrito P, Merran S, Correas JM. How to characterize a solid renal mass: A new classification proposal for a simplified approach. *Diagn Interv Imaging.* 2012;93:232-45.
11. Kovacs G, Akhtar M, Beckwith BJ, Bugert P, Cooper CS, Delahunt B et al. The Heidelberg classification of renal cell tumors. *J Pathol.* 1997;183:131-3.
12. Bosniak MA: Difficulties in classifying cystic lesions of the kidney. *Urol Radiol.* 1991;13:92-3.
13. Ng CS, Wood CG, Silverman PM, Tannir NM, Tamboli P, Sandler CM. Renal cell carcinoma: Diagnosis, staging, and surveillance. *AJR Am J Roentgenol.* 2008;191:1220-32.
14. Motzer RJ, Bander NH, Nanus DM: Renal cell carcinoma. *N Engl J Med.* 1996;335:865-75.
15. Daniel WW Jr., Hartmen GW, Witten DM, Forrow GM, Kelalis PP. Calcified renal masses: *Radiology.* 1972;103:503-8.
16. Merten DF, Kirks DR. Diagnostic imaging of pediatric, abdominal masses. *Pediatr Clin North Am.* 1981;19(3):527-45.
17. Miniati D, Gay AN, Parks KV, Naik-Mathuria BJ, Hicks J, Nuchtern JG et al. Imaging accuracy and incidence of Wilms' and non-Wilms' renal tumors in children. *J Pediatr Surg.* 2008;43(7):1301-7.
18. Fritz GA, Schoellnast H, Deutschmann HA, Quehenberger F, Tillich M. Multiphase multidetector-row CT in detection and staging of

- transitional cell carcinoma of the upper urinary tract. *Eur Radiol.* 2006;16(6):1244-52.
19. Ganeshan D, Iyer R, Devine C, Bhosale P, Paulson E. Imaging of primary and secondary renal lymphoma. *AJR Am J Roentgenol.* 2013;201:712-9.
 20. Cohan RH, Dunnick NR, Leader RA, Baker ME: Computed tomography of renal lymphoma. *J Compute Assist Tomogr.* 1997;14:933-8.
 21. Choyke PL, White EM, Zeman RK, Jaffe MH, Clark LR. Renal metastases: Clinicopathologic and radiologic correlation. *Radiology.* 1987;162:359-63.
 22. Goldman SM, Hartman DS, Fishman EK, Finizio JP, Gatewood OM, Siegelman SS. CT of Xanthogranulomatous pyelonephritis: Radiological and pathological correlation: *AJR Am J Roentgenol.* 1984;142(5):963-9.
 23. Warren MM, Kelalis PP, Utz DC. The changing concept of hypernephroma. *J urol.* 1970;104:3:376-9.

Cite this article as: Thakor DR, Rana YR, Sheth MM. Imaging spectrum of renal masses on multi-slice computed tomography. *Int J Res Med Sci* 2020;8:3657-64.